9.6 EVIDENCE OF LONG EQUATORIAL WAVE REFLECTION FROM TOPEX/POSEIDON SEA-LEVEL DATA

Jean-Philippe Boulanger* and Lee-Lueng Fu

Jet Propulsion Laboratory / California Institute of Technology
Pasadena, California, USA

I. INTRODUCTION

The delayed action oscillator mechanism has been suggested by Schopf and Suarez (1988) to be a potential mechanism for El Niño/Southern Oscillation (ENSO). Using a linearized version of the Cane and Zebiak (1986) coupled model, Battisti (1988) showed that this mechanism was at work in the coupled model, that long equatorial wave propagation and reflection at the Pacific western boundary were necessary conditions for the coupled system to oscillate.

Recently, Li and Clarke (1994), studying historical data, argued that "extra-physics beyond the delayed action oscillator is necessary to describe ENSO". In response, Mantua and Battisti (1994) revisited this mechanism and argued that even if this mechanism cannot explain the lack of regularity of ENSO events, it eventually provides a potential explanation of growth and termination of these events. In particular, western boundary reflection acts mainly as a termination mechanism for warm events.

With the full deployment of the TOGA-TAO (Tropical Ocean-Global Atmosphere - Tropical Atmosphere Ocean: Hayes et al., 1991) mooring array, and the synoptic and dense coverage provided by altimetric satellites (GEOSAT from 1985 to 1989, ERS-1 since the end of 1991, TOPEX/POSEIDON since October 1992), long wave propagation and reflection can now be investigated throughout the tropical Pacific basin.

In this study, we analyzed TOPEX/POSEIDON sea-level data (Fu et al., 1994) over the November 1992-January 1995 period. Standard instrument and environmental corrections (including the inverted barometer correction) were applied to the data (Callahan, 1994). Additionally, the tidal model of Ma et al. (1994) based on TOPEX/POSEIDON data was also applied. Along-track data were binned into a 3° longitude by 0.5° latitude grid for the analysis presented below. Data were filtered with a 50-day Harming filter except when specified. TOPEX/POSEIDON sea-level data were then projected onto long equatorial waves using Boulanger and Menkes (1995)'s decomposition method. Finally, potential reflections at both eastern and western Pacific ocean boundaries were examined.

* *Corresponding author address*:

Jean-Philippe Boulanger, Jet Propulsion Laboratory, MS 300-323, 4800 Oak Grove Drive, Pasadena. CA 911(D, USA: e-mail: jpb@pacific.jpl.nasa.gov

II. LONG WAVE COEFFICIENTS

A detailed description of both Kelvin and first Rossby wave variability is given by Boulanger and Menkes (1995) during the November 1992-December 1993 period. In the following, we only describe the major features. To study wind forcing variability and its potential contribution to long equatorial wave signal, ERS- 1 zonal wind stress data (provided by Dr. David Halpern) were projected onto long wave structures. The calculated forcing coefficients were then integrated along wave characteristics to obtain wave solutions assuming a 2.5m/s baroclinic phase speed. A Rayleigh friction with a 3 month timescale is applied, and the shallow-water upper layer thickness is taken to be 70m. Kelvin and first Rossby sea-level structures are displayed in Figure 1.

Kelvin wave coefficient, Figures 2a and 2b repectively display Kelvin coefficients obtained from the T/P observations (via wave decomposition) and the integration of the ERS- 1 wind forcing.. As already found in previous studies (Delcroix et al., 1994; Kessler and McPhaden, 1995; Boulanger and Menkes, 1995), wind forcing explains most of the wave variability east of 165°E.

Major differences between T/P and ERS- 1 Kelvin coefficients can be observed near the western boundary during the entire period. In particular, from January to November 1993, T/P Kelvin signal in the western Pacific is upwelling (Fig. 2a). However, wind forcing contribution exhibits a stronger variability with alternating upwelling

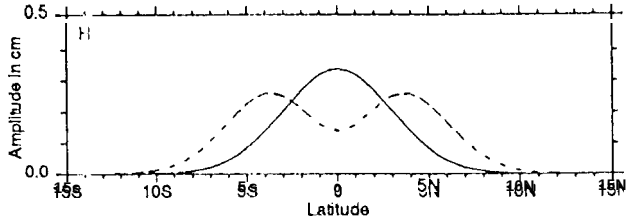

Figure 1: Meridional structures of sea-level for Kelvin and first Rossby modes (calculated for a 2.5 m/s phase speed). Each wave amplitude at a given latitude can be obtained by multiplying the meridional structure to the oceanic coefficient.

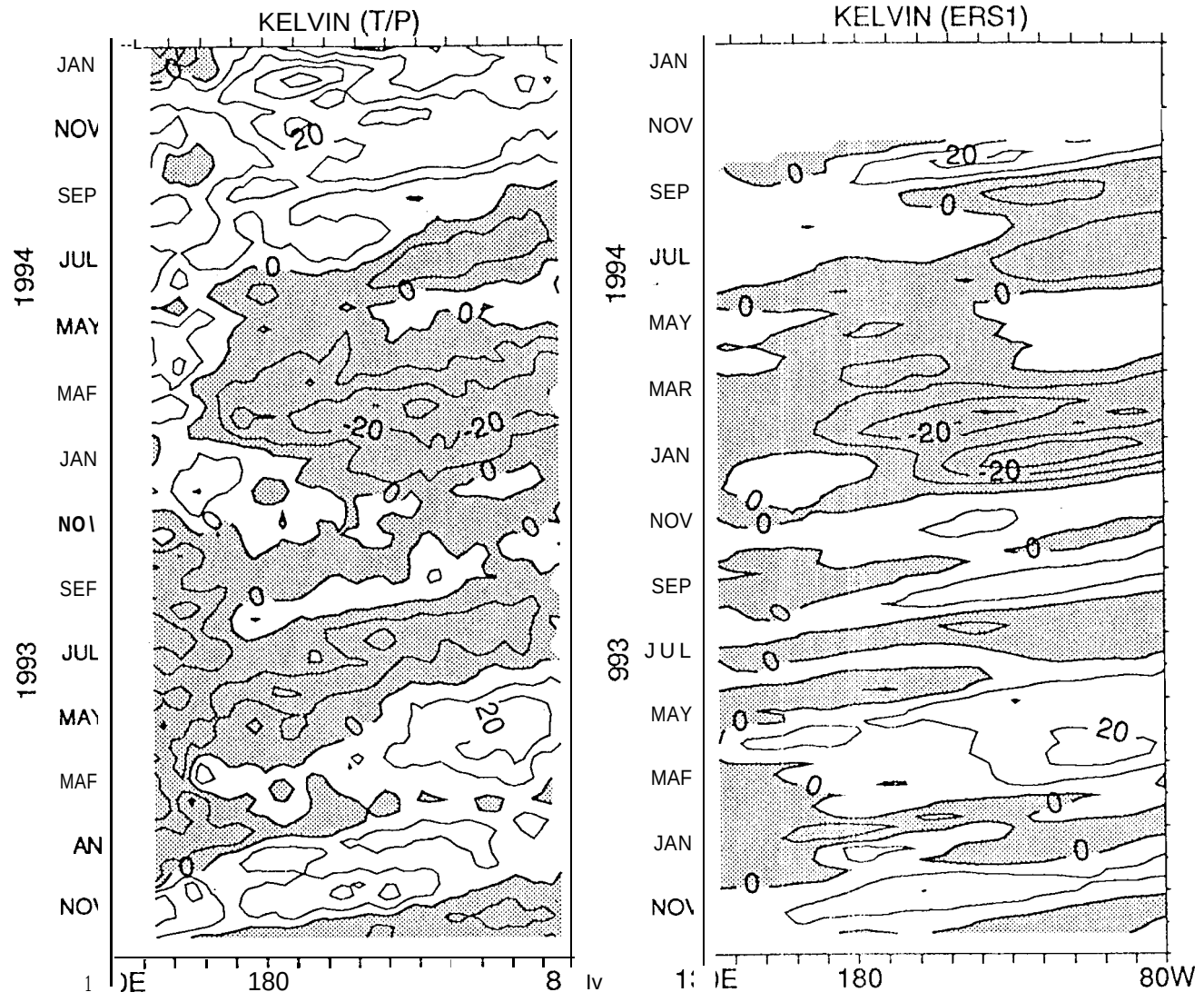

Figure 2: Longitude-time Plots of Kelvin wave coefficient calculated (a: left) from T/I' sea-level data and (b: right) from integration along 'Kelvin wave characteristics of ERS- 1 derived Kelvin forcing. Coefficients are non-dimensionnalised. Contour intervals are every 10 units. and negative values are shaded. An oceanic coefficient of 10 units would yield to an equatorial sea-level amplitude of 3.2 cm.

and downwelling waves (Fig. 2b). Then, in January-March 1994, whale the wind forcing is favorable for up welling Kelvin waves, only downwelling Kelvin waves are observed in the data. After July, although both T/P and ERS- 1 Kelvin coefficients are downwelling, wind forcing contribution is weaker than the observed amplitude. Therefore. during the entire period in the western Pacific region (140°E to 165°E), the wind-forced signal does not explain observed Kelvin wave amplitude. Whether Kelvin wave signal in this region is coming from reflection of Rossby waves at the western boundary will be examined in the following.

First Rossby wave coefficient. Contrary to Kelvin wave coefficient, first Rossby wave coefficient (Fig. 3a-b) displays a strong seasonal cycle: at the beginning of the year, downwelling waves are wind-forced near 140° W; during Spring, when the Trades weaken, a strong upwelling wave is generated from 11 0°W; finally, when the Trades strengthen. another wind-forced downwelling signal is observed from 140°W. However, while changes in the wave amplitudes from 1993 to 1994 seem mainly related to wind forcing variability (Fig. 3b), the observed Rossby signal near the eastern boundary seems rather related to incoming Kelvin waves (compare Figures 2a and 3a) leading to potential reflection of Kelvin waves at the eastern boundary.

III. LONG WAVE REFLECTION

Eastern boundary reflection. Reflections are investigated at two longitudes 84°W and 93°W, respectively located east and west of the Galapagos Islands. If reflec-

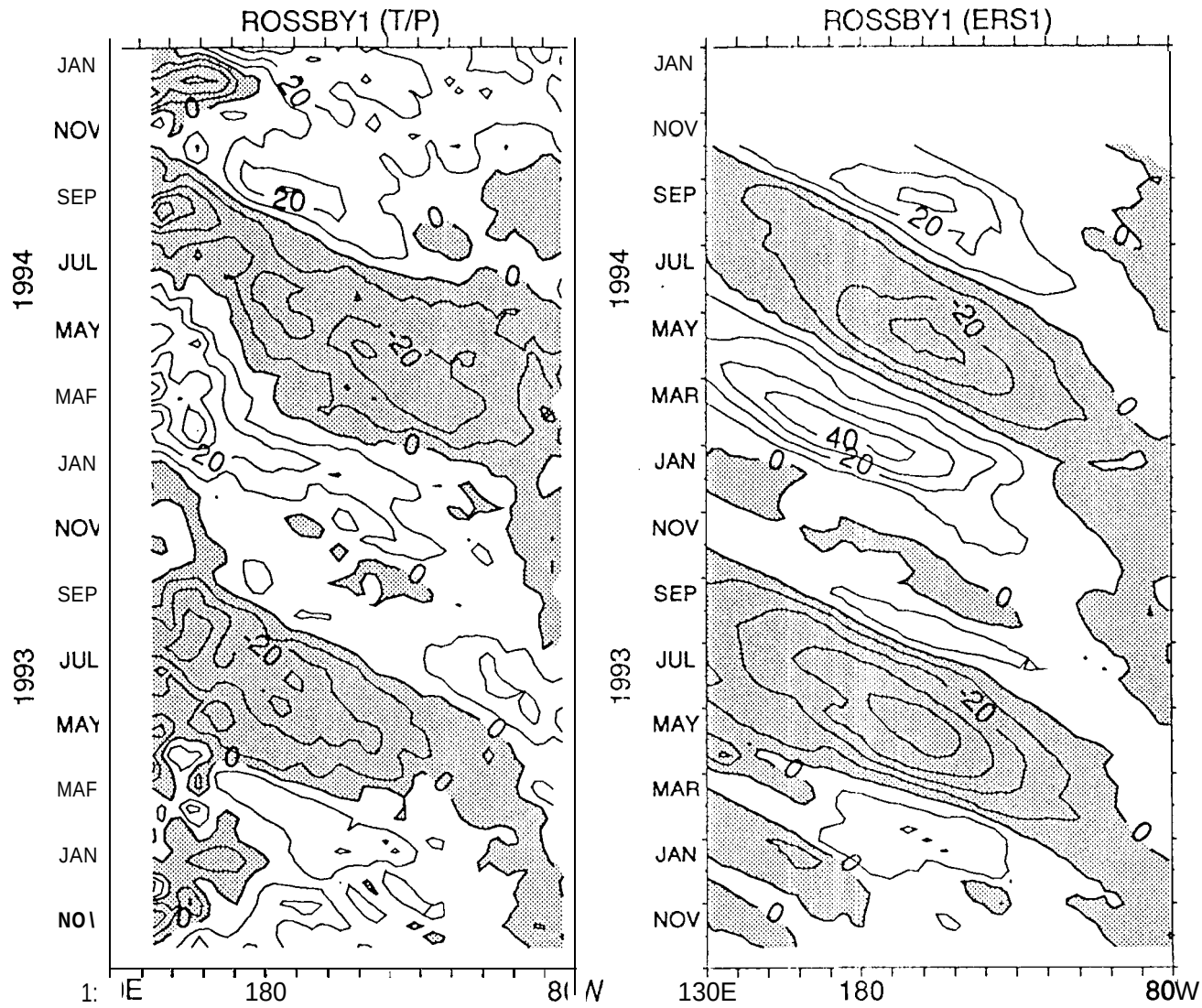

Figure 3: Longitude-time plots of first meridional Rossby wave coefficient calculated (a: left) from T/P sea-level data and (b: right) from integration along first Rossby wave characteristics of ERS-1 derived first Ross by forcing. Coefficients are non-dimensionnalised. Contour intervals are every 10 units. and negative values are shaded. An oceanic coefficient of 10 units would yield to a sea-level amplitude at 4°N of 2.8 c-m.

tions occur at 80°W, the time for a first baroclinic mode Kelvin wave at 84°W (93°W) to propagate to and reflect at the coast and to travel back as a first meridional Rossby wave would be 10 days (30 days). First, we compared Kelvin and first Rossby wave coefficients at both longitudes, and we found that they were correlated at 0.78 at 84°W and 0.64 at 93°W. When T/P Kelvin wave coefficient is shifted by the corresponding lag. correlation increased respectively to 0.85 and 0.81. The ratio of first Rossby to Kelvin standard deviations during the period under study is equal to 1.0 at 84°W and 0.8 at 93"W. The first value would indicate that the reflection efficiency of South America coasts is 80% of that of an infinite meridional wall.

To investigate the variation of wave amplitudes from 84° W to 94°W, Kelvin (first Rossby) time series at both locations are plotted in Figure 4c (4d). Kelvin wave coefficients are correlated at 0.90, and no significant difference is observed in the Kelvin signals east and west of the Galapagos Islands. However, first Rossby wave coefficients are cori elated at 0.79, and standard deviation west of Galapagos Islands is 20% weaker than east. As wind forcing contribution in this region is rather weak (Fig. 3b), the drop in Rossby wave amplitude could be due to the vertical energy propagation described by Kessler and McCreary (1993).

Western boundary reflection. Boulanger and Menkes (1995) showed that the accuracy in the decomposition calculation in terms of Kelvin and first Rossby wave amplitudes is getting higher when data southern boundary is southward of 2"S. Therefore, we studied reflection at the western boundary by investigating potential relationship

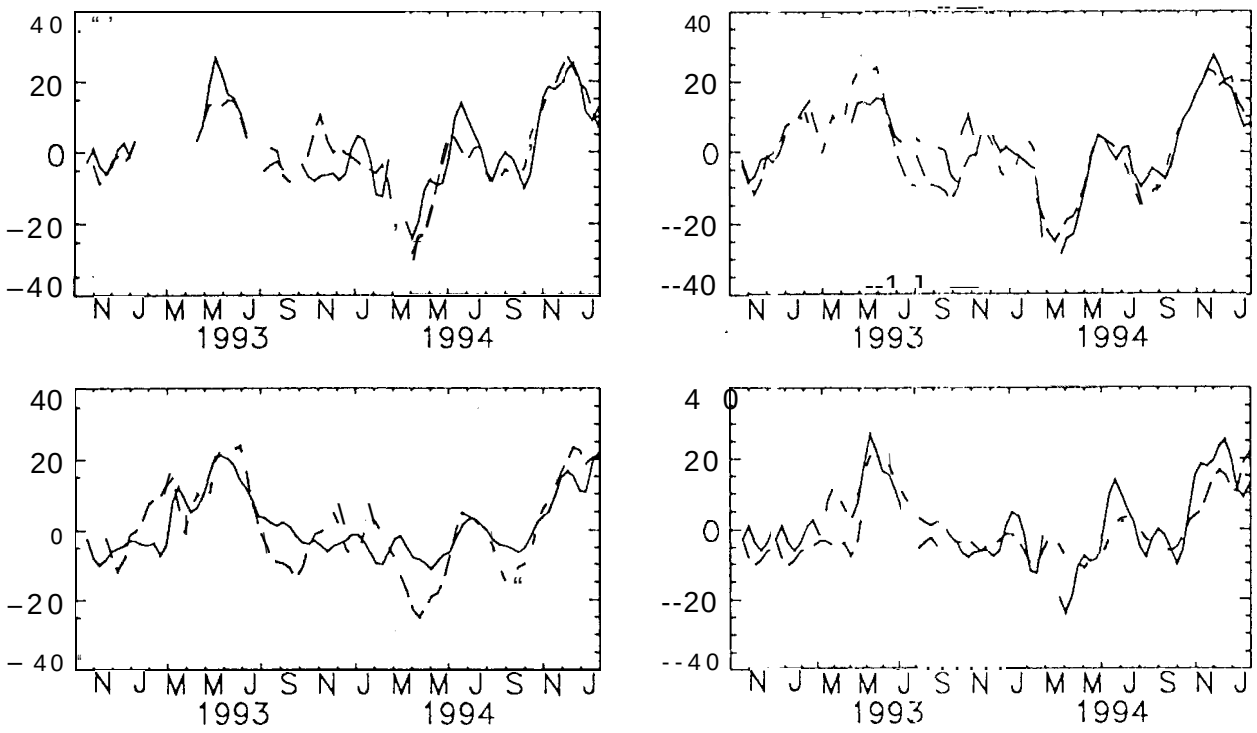

Figure 4: (a top-left) T/P Kelvin wave coefficients at 84°W shifted by 10 days (solid lime) and T/P first Rossby wave coefficient at 84°W; (b: bottom-left) same as (a) but at 93° W; (c: top-right) TIP Kelvin coefficient at 84°W (solid line) and at 93"W (dashed line); (d bottom-right) same as (c) but T/P first Rossby wave coefficient.

between Kelvin and first Rossby wave coefficients at 144°E (Fig. 5). Due to a possible bias by tides at 60-day period (aliased M2 period in T/P data) in this region of complex topography, we decided to filter data by a 90-day Harming filter. Assuming a 2.5m/s baroclinic phase speed, the time for a first meridional Rossby wave to propagate from 144°E to 130°E, to reflect and to travel back to 144°E as a Kelvin wave is around 30 days. Correlation between Kelvin and first Rossby coefficients is 0.27. When shifting the first Rossby coefficient by 30 days, it is improved to 0.53. However, except for the January-July 1994 period, no clear coherency can be observed between both coefficients. When correlation is calculated only during these first months of 1994. correlation is found equal to 0.92. One must keep in mind that this period is short, and that our filter length is long so that confidence level of this correlation value is not much higher than 80%. However, it confirms that the downwelling Kelvin signal, previously observed in Figure 2a in the western Pacific during the January-July 1994 period and not explained by wind variability (Fig. 2b) is indeed related to propagating downwelling Rossby wave-s forced near the dateline. During this period, the ratio between Kelvin and first Rossby wave standard deviations is around 0.6, while theory would predict 0,4 if the boundary is a meridional wall infinite to the north and bounded at the equator. Our result is roughly consistent with theory.

Previous results show that Kelvin wave signal in the western Pacific (west of 165°E) during the frost months of 1994 can be explained by first Rossby wave reflection. However, during the rest of the period observed by the TOPEX/POSEIDON altimeter, neither wind forcing nor first meridional Rossby mode reflection can explain Kelvin wave variability and amplitude. Whether it comes from higher Rossby modes, partial reflections at Papua-New Guinea coasts as Rossby waves propagate westward, or other mechanisms (throughflow, non-linearity,...) is not yet understood.

IV. CONCLUS1ON

TOPEX/POSEIDON (T/P) sea-level data were used to investigate long wave reflection at both eastern and western boundaries during the more than 2-year period of observations now avail able . The aim of the present work

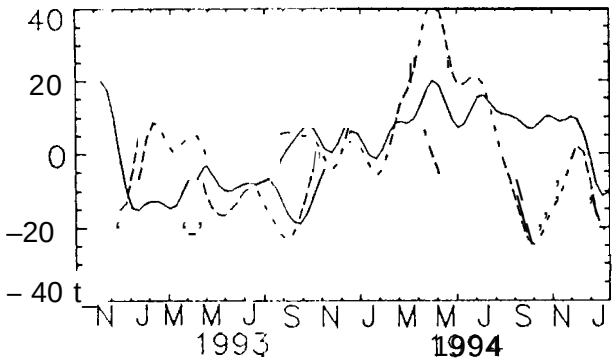

Figure 5: T/p Kelvin wave coefficients (solid line) and first Rossby wave coefficients shifted by 30 days (dashed line) at 144°E. Time series are filtered by a 90-day Harming filter.

was to assess the reflection hypothesis of the delayed action oscillator (Battisti, 1988; Mantua and Battisti, 1994).

Following Boulanger and Menkes (1995)'s decomposition method, T/P sea-level data were projected onto long equatorial wave structures. In this study, we only focused on Kelvin and first Rossby waves during the November 1992-January 1995 period. We first observed that Kelvin wave variability is different from 1993 to 1994, and that most of it could be explained by wind variations west of 165°E. However, Kelvin wave amplitude near the western boundary can not be fully explained by wind forcing. In particular, in January-July 1994, strong downwelling Rossby waves were propagating westward, while later downwelling Kelvin waves were observed in this region. Despite interannual changes in amplitude, first Rossby wave signal is found to be strongly dominated by an annual cycle. Downwelling waves are first generated in the beginning of the year near 140°W. Then, while the Trades weaken, a strong upwelling signal is observed. Later downwelling waves are forced by strengthening of the Trades. Strong variability in the wave amplitude is observed from 1993 to 1994. Besides, wind variability does not explain Rossby signal in the eastern Pacific region. It appears indeed to be related to impinging Kelvin waves at the eastern boundary. Both boundaries are then examined.

At the eastern boundary, Kelvin waves were actually reflecting into first Rossby during the entire period. The reflection efficiency of South America coasts is estimated to be 80%0 of that of an infinite meridional wall. While no significant differences are observed in Kelvin variability and amplitude west and east of Galapagos Islands, Rossby wave amplitude is dropping by 20% when propagating from 84°W to 93°W. This feature could be explained by a vertical energy propagation mechanism (Kessler and McCreary, 1993).

The delayed action oscillator theory is based on interannual time scale propagation and reflection of Kelvin and first Rossby waves. Satellite time coverage is too short to extract seasonal cycle, therefore our sea-level data are relative to a January 1993-December 1994 two-year mean. Although we did not observe any reflection of upwelling Rossby waves at the end of the warm 1992-1993 ENSO, we observed reflections of downwelling first Rossby waves during the January-July 1994 period prior to the warming observed in late 1994. Whether the lack of other reflection is due to our d ata set, to the period under study or to a dependence of reflection occurence on oceanic conditions in the western Pacific will have to be investigated. Moreover, the actual role of long equatorial waves on sea surface temperature will have to be studied for supporting the role hypothesized in the delayed action oscillator theory.

VI. REFERENCES

Battisti, D. S., 1988: Dynamics and thermodynamics of a warming event in a coupled tropical atmosphere-ocean model. *J. Atmos. Sci., 45,2889-2819.*

Boulanger, J.-P., and C. Menkes, 1995: Propagation and reflection of long equatorial waves in the Pacific ocean during the 1992-1993 El Niño. *J. Geophys. Res.*, accepted.

Callahan, P. S.. 1994: Topex/Poseidon Project GDR Users Handbook, JPL D- 8944 (internal document), rev A, Jet Propulsion Laboratory, Pasadena, Calif., 84 pp.

Delcroix, T., J.-P. Boulanger, F. Masia, and C. Menkes, 1994: GEOSAT-derived sea-level and surface current anomalies in the equatorial Pacific during the 1986-1989 El Niño and La Niña *J. Geophys. Res., 99,25093-25107.*

Fu, L.-1,., E. J. Christensen, C. Yamarone, M. Lefebvre, Y. Menard, M. Dorrer, and P. Escudier, 1994: TOPEX/POSEIDON Mission Overview. J. Geophys. Res., 99,24369-24381.

Hayes, S. P., L. J. Mangum, J. Picaut, A. Sumi, and K. Takeuchi, 1991: TOGA-TAO: A morred array for real-time measurements in the tropical Pacific ocean. *Bull. Am. Met. Sot., 72,3,339-347.*

Kessler, W. S., and J. P. Mccreary, 1993: The annual wind-driven Rossby wave in the subthermocline equatorial Pacific. *J. Phys. Oceanogr., 23,* 1192-1207.

Kessler, W. S., and M. J. McPhaden, 1995: Oceanic equatorial waves and the 1991-1993 El Niño. *J. Climate, S, 1757-1774.*

Li, B., and A. J. Clarke, 1994: An examination of some ENSO mechanisms using interannual sea-level at the eastern and western equatorial boundaries and the zonally averaged equatorial wind. *J. Phys. Oceanogr., 24, 681-690.*

Ma, X. C., C.K. Shum, R.J. Eanes, and B.D. Tapley, 1994: Determination of ocean tides from the first year of TOPEX/POSEIDON altimeter measurements, J. Geophys. Res., 99,2.4809-24820.

Mantua, N. J., and D. S. Battisti, 1994: Evidence for the delayed action oscillator mechanism for ENSO: The "observed" oceanic Kelvin mode in the far western Pacific. *J. Phys. Oceanogr., 24,691-699.*

Menkes, C., J.-P. Boulanger, and A. J. Busalacchi, 1995: Evaluation of TOPEX and basin-wide TOGA-TAO sea-level surface topographies and derived geostrophic currents. *J. Geophys. Res.*, accepted.

Schopf, P. S., and M. J. Suarez, 1988: Vacillations in a coupled ocean-atmospjere model. *J. Atmos. Sci., 45, 549-566.*

Zebiak, S. E.. and M. A. Cane, 1987: A model of El Niño/Souterhn Oscillation. *Mon. Wea. Rev., 115, 2262-2278.*